

Observation and Analysis of Maser Activity in a Tokamak Plasma

R. F. Gandy,^(a) I. H. Hutchinson, and D. H. Yates

Plasma Fusion Center, Massachusetts Institute of Technology, Cambridge, Massachusetts 02139

(Received 1 October 1984)

High-resolution spectral measurements of electron plasma-frequency emission from Alcator *C* tokamak reveal a level of coherence indicative of maser activity ($\Delta\omega/\omega = 6 \times 10^{-6}$). A full-wave theoretical analysis yields the complete mode structure of the electromagnetic fields as well as the dispersion relation. This analysis shows that for wave frequencies near the central plasma frequency the waves are highly localized and thereby the plasma forms a high-*Q* cavity for these waves.

PACS numbers: 52.25.Sw, 42.52.+x

Extremely intense radiation indicative of collective nonthermal emission processes is observed in a variety of laboratory and astrophysical plasmas¹ and its detailed understanding remains a key area of plasma physics. In toroidal plasma experiments such as tokamaks, emission is often observed near the electron plasma frequency.²⁻⁵ The emission is of at least two types: quiescent, above the central plasma frequency, which has been interpreted^{6,7} as due to spontaneous Cherenkov emission into the slow extraordinary mode; and fluctuating, which is the subject of the present study. Our results lead us to the clear inference that this fluctuating or "bursting" emission is due to coherent maser action, in which the plasma itself acts as both the high-*Q* cavity and the gain medium. In this Letter, we present high-resolution spectral measurements of the fluctuating ω_{pe} emission from the Alcator *C* tokamak, which reveal the highly coherent nature of the emission. We have carried out a theoretical linear, electromagnetic analysis of the wave properties for monotonically decreasing electron density and finite magnetic field. The results of the calculations indicate that centrally localized wave fields exist. This central trapping of the wave forms the basis of the maser action experimentally observed.

Previous measurements^{3,4} revealed that the fluctuating emission from Alcator occurred at a frequency within 5% of the central plasma frequency, ω_{pe0} (the 5% representing the uncertainty in the independent determination of central density), and that the linewidth of the spectral feature was narrow but unresolved ($\Delta\omega/\omega \leq 10^{-3}$). The bursting ω_{pe} emission is commonly observed during the early portion of the plasma pulse and immediately after the shutdown of lower-hybrid current drive.⁸ Other observations (e.g., soft and hard x rays) confirm that the emission is contingent upon the presence of a high-parallel-energy tail on the electron distribution (runaway electrons), but the tail is not sufficient. For example, bursts are never seen during current drive even though a tail is present.

The radiation bursts have a very rapid rise time, approximately 1 μ s. They typically last 5–10 μ s. Radiation temperatures exceed 10^5 eV and total emitted

power in a burst is of order 100 W, though precise estimates of emitted power are impossible because of the restricted viewing geometry on Alcator *C*.

Observations have been made with four heterodyne radiometers having center frequencies of 31, 43, 61, and 87 GHz. Bursts are observed on a radiometer only when the central plasma frequency is within a few gigahertz of the radiometer frequency. For example, as density rises the bursts appear sequentially, first in the lower- and then in the higher-frequency channels. We present here data from the 61-GHz radiometer, in which, with appropriate image rejection filtering, a typical intermediate frequency (IF) range of 400 to 1500 MHz corresponds uniquely to a microwave frequency range of 61.4 to 62.5 GHz. The IF signal is subsequently amplified and all spectral measurements are made through analysis of the IF signal.

In order to examine a relatively wide range of IF frequencies (approximately 300 MHz) at high resolution (13 MHz), a surface-acoustic-wave (SAW) dispersive delay line was used to make real-time spectral measurements of the fluctuating ω_{pe} emission.⁹ The results from the SAW system indicate a wide variety of power spectra. Single-peak and multiple-peak structures are seen. Almost all individual features are unresolved with a full width at half maximum of 13 MHz, the instrumental resolution. Analysis of the peak-to-peak frequency spacing of the multiple bursts revealed no apparent regularity. The conclusion to be drawn from the SAW system is that a burst is composed of one or more irregularly spaced narrow spectral features. The observation that the individual features were generally unresolved by the SAW led us to employ a higher-resolution technique.

In this technique we take a filtered portion of the IF signal from the microwave mixer (435–447 MHz) and pass it through a second mixer operating with a local oscillator frequency of 435 MHz. Therefore, after the second mixer, the microwave signal range 61.435–61.447 GHz has been transformed to dc–12 MHz. This output signal is directly sampled with a 32 MHz analog-to-digital converter which is typically clocked for 5- μ s time duration (approximate duration of a

burst). The sampled data are Fourier transformed to obtain the power spectrum, whose spectral resolution, determined by the time duration (transform limited), is generally ≤ 200 kHz.

Spectral widths in the range 400–800 kHz are observed. One of the narrower features is shown in Fig. 1 (full width at half maximum of 420 kHz). Another interesting feature is a frequency shift during certain bursts. This shift can be seen in the time-domain data [Fig. 2(a)] and in the transformed spectrum [Fig. 2(b)]. These frequency shifts are possibly related to changes in longitudinal-mode number and will be discussed later.

The theoretical cavity mode structure for waves near ω_{pe} may be obtained from an analysis taking the plasma to have cylindrical symmetry, and using the cold-plasma dielectric tensor. Taking the applied magnetic field to be purely axial ($\mathbf{B}_0 = \hat{z}B$), we seek solutions to Maxwell's equations proportional to $\exp[i(kz + m\theta - \omega t)]$, and which satisfy appropriate boundary conditions. The equations can be reduced to two second-order equations¹⁰ for the perturbed fields E_z and B_z which are coupled by the plasma anisotropy and inhomogeneity. These may be solved numerically, but for the case of interest, in which $\omega/\Omega \ll 1$ ($\Omega \equiv eB/m$) and $c/\omega_p a \ll 1$ (where a is the plasma radius) an accurate analytic approximation is possible. In this case, the equations decouple to second order in these small parameters and the E_z mode (TM mode), which has frequency just below the central plasma frequency ω_{p0} , and which corresponds approximately to the slow ordinary (whistler) branch of the homogeneous plasma

dispersion relation, exhibits centrally localized solutions, trapped near the density maximum. Because of this localization, one can express the density profile as the (parabolic) first two terms of its Taylor expansion: $\omega_{pe}^2 = \omega_{p0}^2(1 - r^2/a^2)$ and take the boundary condition to be $E_z \rightarrow 0$ as $r \rightarrow \infty$. The cavity modes are unaffected by the precise plasma edge conditions.

The E_z equation then becomes¹¹

$$\left(\frac{1}{r} \frac{d}{dr} r \frac{d}{dr} - \frac{m^2}{r^2} + \mu^2(\lambda^2 - r^2) \right) E_z = 0,$$

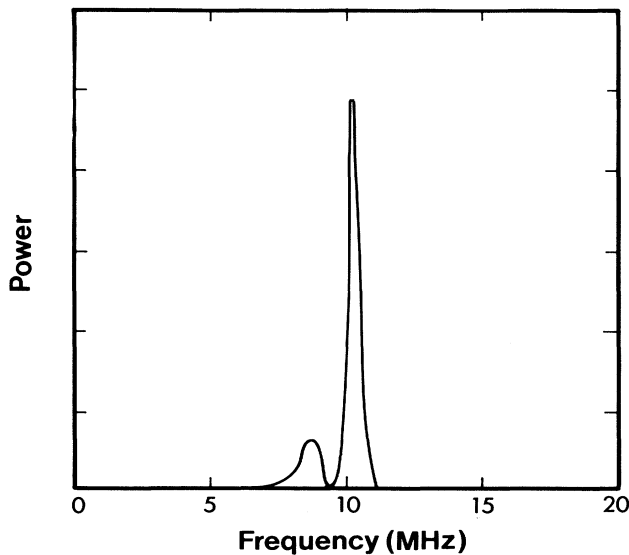


FIG. 1. Power spectrum of bursting ω_{pe} emission. The frequencies have been downconverted by 61.435 GHz. The feature centered at 10 MHz has a full width at half maximum of 420 kHz.

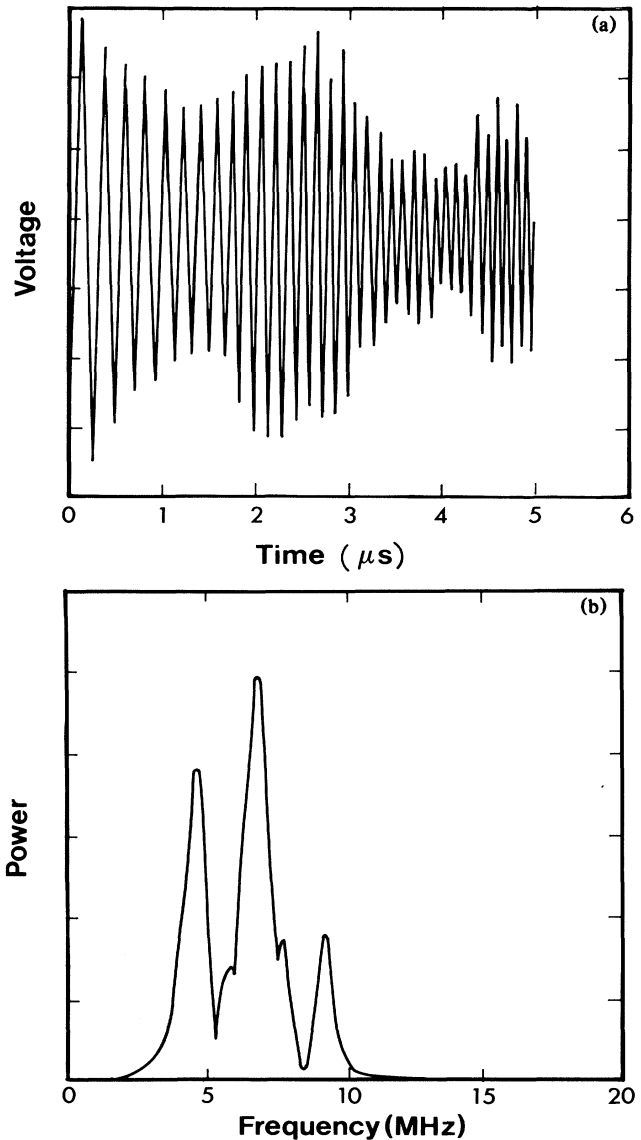


FIG. 2. (a) Raw data from direct sampling method. Note the shift to higher frequency as time increases. (b) Power spectrum of data shown in 2(a). Triplet spectral feature is revealed.

where

$$\mu^2 = \frac{X_0 \omega_{p0}^2}{a^2 c^2} \frac{(N^2 - 1)^2 - N^4 / Y^2}{N^2 - 1},$$

$$\lambda^2 = \frac{a^2 (X_0 - 1)}{X_0} - \frac{c^2 2mN^2}{\omega_{p0}^2 Y (N^2 - 1)},$$

$X \equiv \omega_{pe}^2 / \omega^2$, $Y = \Omega / \omega$, $N = kc / \omega$, and subscript zero indicates central value. The solutions of this equation

$$\omega = \omega_{p0} \left[1 - \frac{2(2n + m + 1)}{\omega_{p0} a / c} \left(\frac{N^2 - 1}{(N^2 - 1)^2 - N^4 / Y^2} \right)^{1/2} \left(1 - \frac{2mN^2}{(2n + m + 1)(N^2 - 1)^{3/2} Y \omega_{p0} a / c} \right)^{1/2} \right]^{1/2},$$

which shows that the eigenfrequency is slightly below the central plasma frequency.

In Fig. 3, we show the wave mode structure of the three lowest-order eigenmodes for plasma parameters typical of the Alcator C experiments, and parallel refractive index $N = 1.3$. The modes are, as anticipated, highly localized near the axis, $r = 0$; for slower waves, $N > 1.3$, this localization is even more pronounced. This central trapping is essential for masing to occur.

Thermal effects can be taken into account¹¹ in the real part of the frequency in the form of Bohm-Gross dispersion by multiplying the above mode frequency by $(1 + 3N^2 v_i^2 / c^2)^{1/2}$. The gain of the medium, i.e., the imaginary part of the frequency, ω_i , depends on the details of the electron distribution function. "Cherenkov" (Landau) gain arising from the wave particle resonance at $\omega = k_{\parallel} v$ requires a positive slope on the parallel distribution function and the growth

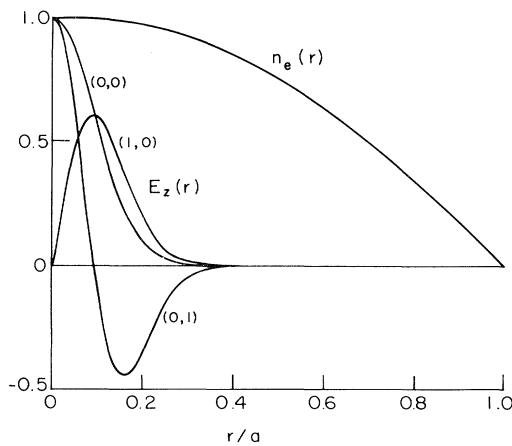


FIG. 3. Three lowest-order solutions (m, n) to E_z eigenmode equation vs normalized plasma radius, for plasma parameters appropriate to the experimental results: $\Omega / \omega = 5$, $\omega_p a / c = 160$, and $N = 1.3$. Also shown is the assumed parabolic density profile.

are

$$E_z = L_n^m(\mu r^2) (\mu r^2)^{m/2} \exp(-\mu r^2 / 2),$$

where L_n^m is the associated Laguerre polynomial. The mode number n , which must be integral to satisfy the boundary condition at ∞ , is given by the equation

$$\lambda^2 \mu = 2(2n + m + 1),$$

which is the required dispersion relation linking ω and N for given m and n . It may be solved to give

rate is approximately the same as for a homogeneous plasma:

$$\omega_i \simeq \frac{\pi}{2} \frac{c^2}{N^2} \left. \frac{df}{dv_{\parallel}} \right|_{c/N} \omega_r$$

(with small corrections for the inhomogeneity¹¹). The positive value of the df/dv_{\parallel} corresponds to the population inversion in the maser. It is believed to arise from the pitch-angle scattering of electrons by waves arising from the anomalous cyclotron-resonance (Parail-Pogutse) instability.¹²⁻¹⁴ Therefore, one can think of these latter waves as being the "pump" of the maser. The highest growth rate for a given N generally occurs for the lowest-order (m, n) mode. The most unstable N occurs near the maximum of df/dv_{\parallel} .

The longitudinal group velocity, v_g , of the waves can be deduced from the previous formulas and enables a calculation of the longitudinal-mode spacing $\Delta\omega$ of the cavity to be obtained, $\Delta\omega = v_g / R$, where R is the major radius (0.64 m for Alcator C). If the multiplet structure of Fig. 2 is interpreted as due to shifting between adjacent longitudinal-mode numbers, the v_g equation allows us to deduce the parallel index of refraction, N , from the experimentally observed frequency shift. For the example presented in Fig. 2, a value of $N = 1.3$ is found, which corresponds to a resonant longitudinal electron energy of 300 keV.

The transverse-mode spacing is much larger, typically ~ 400 MHz, and may explain the occasional occurrence of larger frequency shifts. The "output coupling" mechanism of this maser is still uncertain. The mode structures calculated indicate that the field at the plasma edge is quite negligible for typical parameters and toroidal effects are weak. Therefore, some form of scattering from unknown density perturbations must probably be invoked¹⁵ to account for the observed free-space radiation.

In summary, high-resolution spectral measurements of fluctuating ω_{pe} emission from Alcator C demonstrate a highly coherent maser action. Analysis of

wave structure in bounded plasma for appropriate parameters reveals centrally trapped waves. This trapping explains how the plasma can naturally form the high- Q cavity required for masing and provides the quantitative relationship between the cavity wave frequency and the central plasma frequency.

This work was supported by U.S. Department of Energy under Contract No. DE-AC02-78ET51013.

^(a)Present address: Physics Department, Auburn University, Auburn, Ala. 36849.

¹See e.g., K. Papadopoulos and H. P. Freund, *Space Sci. Rev.* **24**, 511 (1979).

²A. E. Costley and TFR Group, *Phys. Rev. Lett.* **38**, 1477 (1977).

³I. H. Hutchinson and D. S. Komm, *Nucl. Fusion* **17**, 1077 (1977).

⁴I. H. Hutchinson and S. E. Kissel, *Phys. Fluids* **23**, 1698 (1980).

⁵I. H. Hutchinson and S. E. Kissel, *Phys. Fluids* **26**, 310 (1983).

⁶H. P. Freund, L. C. Lee, and C. S. Wu, *Phys. Rev. Lett.* **40**, 1563 (1981).

⁷K. Swartz, I. H. Hutchinson, and K. Molvig, *Phys. Fluids* **24**, 1689 (1981).

⁸M. Porkolab *et al.*, *Phys. Rev. Lett.* **53**, 450 (1984).

⁹R. F. Gandy and D. H. Yates, to be published.

¹⁰E.g., W. P. Allis, S. J. Buchsbaum, and A. Bers, *Waves in Anisotropic Plasmas*, MIT Press Research Monographs, No. 17 (MIT Press, Cambridge, Mass., 1963).

¹¹I. H. Hutchinson and R. F. Gandy, to be published.

¹²V. V. Parail and O. P. Pogutse, *Fiz. Plazmy* **2**, 228 (1976) [*Sov. J. Plasma Phys.* **2**, 125 (1976)].

¹³C. S. Liu *et al.*, *Phys. Rev. Lett.* **39**, 701 (1977).

¹⁴K. Molvig, M. S. Tekula, and A. Bers, *Phys. Rev. Lett.* **38**, 1404 (1977).

¹⁵I. H. Hutchinson, K. Molvig, and S. Y. Yuen, *Phys. Rev. Lett.* **38**, 1404 (1977).